Abstract for 28th IWWWFB, Marseille, France, 2013

Time-domain Hydro-elastic dynamic analysis of a large floating body including second-order wave loads

H.Y. Kang and M.H. Kim
Ocean Engineering Program, Dept. of Civil Eng, Texas A&M University
College Station, Texas, USA
Email: hykang@tamu.edu and m-kim3@tamu.edu

INTRODUCTION

With increasing demands for energy and goods, various types of floating structures face expansion of scale and working environment, i.e. extended spar or TLP for ultra-deep water, various offshore platforms for arctic, very large container ships, multiply connected floating breakwaters and wave energy converters. Corresponding to the expansion of scale and environment, the floating structures are exposed to various problems including resonance, which is induced by deformation of the body and it's interaction with waves or any other offshore loadings such as iceberg impact.

To resolve the elastic floating body interaction, several methods were suggested: modal expansion method for linear waves and direct simulations using FEM-BEM or FEM-FEM combinations. Considering that resonance normally occurs at a couple of lowest elastic modes, second order analysis may be required to account for the resonance induced by sum-frequency wave force. Contrary to full coupling effect by direct simulation, the corresponding computing cost and accuracy issue could be drawbacks of the direct simulation.

As an initiating work to achieve complete second order hydroelastic analysis on time domain, a fully coupled time-domain hydro-elastic dynamic analysis is addressed, based on modal expansion method to couple with elasticity and Volterra series method to apply second order wave induced loading. The methodology can be extended to various applications for irregular waves such as additional coupling with mooring system or impact loadings, even with dramatically reduced computing cost. In addition, it can generate instantaneous irregular wave-induced loadings acting on the floating body as time series, which can be used for global and local stress analysis.

FORMULATION

To account for interactions of body deformation, a finite series of elastic modes is regards as sufficient basis to represent the deformation. In further, the elastic modes are applied to a general boundary value problem as additional modes to solve with rigid body's six degree of freedom. For the extended modes of elasticity, inertia and stiffness components can be obtained by modal analysis, based on diagonalization by eigenfunction.

Assuming a pontoon type floating body as Euler-Bernoulli Beam in Eq. 1, analytic solution of mode shapes is given and one can get diagonalized modal inertia, stiffness, and excitation for the modes. A few simple geometries have analytic solutions of mode shapes. For arbitrary body, one may get approximate modal results from a FEM program.

$$\frac{\partial}{\partial x^2}\left(EI\frac{\partial^2 w}{\partial x^2}\right)+m\frac{\partial^2 w}{\partial t^2}=q(x)r(t)$$

$$w(x,t)=\sum_{k=1}^{\infty}a_k(t)\varphi_k(x) \qquad \textit{where } \varphi_k(x) \text{ is } k^{th} \text{ mode shape function.} \tag{1}$$

$$\int_x m\varphi_k^{\,2}(x)dx\cdot\ddot{a}_k(t)+\int_x EI\varphi_k''''(x)\varphi_k(x)dx\cdot a_k(t)=\int_x q(x)\varphi_k(x)dx\cdot r(t) \quad \textit{where } k=1,...,e$$

With the additional elastic modes, boundary value problem is extended for body surface boundary condition to the elastic modes e.

$$\nabla^2\phi^{(1)} = \nabla^2(\phi_D{}^{(1)} + \phi_R{}^{(1)}) = 0 \qquad \text{in fluid domain}$$

$$where\ \phi_D{}^{(1)} = \phi_I{}^{(1)} + \phi_S{}^{(1)},\ and\ \phi_R{}^{(1)} = \sum_{k=1}^{K}\zeta_k\phi_k{}^{(1)},\ K = 6+e$$

$$\frac{\partial\phi^{(1)}}{\partial z} - \kappa\phi^{(1)} = 0 \quad on\ z=0, \quad and\ \frac{\partial\phi^{(1)}}{\partial z} = 0 \quad on\ z=-h, \tag{2}$$

$$\frac{\partial\phi_R{}^{(1)}}{\partial n} = i\omega n\cdot(\xi + \alpha\times r + \varphi), \quad \frac{\partial\phi_D{}^{(1)}}{\partial n} = 0 \quad on\ S_w$$

Based on the fully coupled hydro-elastic dynamic coefficients and hydrostatic revision due to elastic motions (Kang et al., 2012), time domain hydro-elastic dynamic analysis is developed from Kramers-Kronig relation.

$$(M_{ij} + \Delta M_{ij}^{\infty})\ddot{X}_j + (K_{ij}^E + K_{ij}^H)X_j = F_i^{(1)}(t) + F_i^{(2)}(t) + F_i^C(t) + F_i^D(\mathrm{t})\ where\ i,j = 1,\ldots,6+e$$

$$\Delta M_{ij}^{\infty} = \Delta M_{ij}(\omega_{\max}) + \int_0^{\infty} R_{ij}(t)\frac{\sin(\omega_{\max}t)}{\omega_{\max}}dt \qquad where\quad R_{ij}(t) = \frac{2}{\pi}\int_0^{\infty}B_{ij}(\omega)\cos(\omega t)d\omega \tag{3}$$

$$F_i^C(t) = -\int_{-\infty}^{t} R_{ij}(t-\tau)\dot{X}_j(\tau)d\tau = -\int_{-t}^{\infty} R_{ij}(\tau)\dot{X}_j(t-\tau)d\tau = -\int_0^{\infty} R_{ij}(\tau)\dot{X}_j(t-\tau)d\tau$$

Comparing with rigid body time domain analysis, matrix size is extended to $6+e$, and coupling effects between elastic motions and rigid motions are given in terms of off-diagonal elements in inertia and hydrostatic matrices, and convolution integrals.
Considering that first several elastic modes normally have natural frequencies outside of linear wave spectrum but within range of sum-frequency excitations, it would be needed to apply second order wave induced loadings into the hydro-elastic analysis. Under an assumption of small wave slope, perturbation method is utilized to solve the second order wave-body interaction problem (Molin, 1979 and Kim and Yue, 1989 and 1990). The boundary value problem is given in Eq. 4, based on Kim and Yue 1990. Similarly to first order boundary value problem, main difference between rigid body analysis and elastic body analysis in second order is also body boundary condition.

$$\nabla^2\phi_D^{(2)} = 0 \qquad \text{in fluid domain,}$$

$$\left(\frac{\partial}{\partial t^2} + g\frac{\partial}{\partial z}\right)\phi_D^{(2)} = \left[\frac{1}{g}\frac{\partial\phi^{(1)}}{\partial t}\frac{\partial}{\partial z}\left(\frac{\partial^2\phi^{(1)}}{\partial t^2} + g\frac{\partial\phi^{(1)}}{\partial z}\right) - \frac{\partial}{\partial t}\left(\nabla\phi^{(1)}\right)^2\right]$$
$$-\left[\frac{1}{g}\frac{\partial\phi_I^{(1)}}{\partial t}\frac{\partial}{\partial z}\left(\frac{\partial^2\phi_I^{(1)}}{\partial t^2} + g\frac{\partial\phi_I^{(1)}}{\partial z}\right) - \frac{\partial}{\partial t}\left(\nabla\phi_I^{(1)}\right)^2\right] \quad \text{on free surface} \tag{4}$$

$$\frac{\partial\phi_D^{(2)}}{\partial n} = -\frac{\partial\phi_I^{(2)}}{\partial n} + n\cdot B$$, where B is second order body boundary velocity including elasticity.

Starting with second order radiation potential problem for elastic body by separation from combined body boundary condition above, one can find that the formulas for the radiation potential-induced hydro-elastic dynamic coefficients are identical between first and second order because of similar form of boundary condition. However, the relevant frequency $\omega^{(2)}$ is different and it presents sum and difference frequencies of bichromatic incident waves.

$$\frac{\partial\phi_R{}^{(2)}}{\partial n} = i\omega^{(2)}n\cdot(\xi^{(2)} + \alpha^{(2)}\times r + \varphi^{(2)}) \quad on\ S_w \tag{5}$$

Therefore, for the second order hydro-elastic dynamic analysis in time domain, added mass for infinite frequency and convolution integral terms are same as ones in linear order analysis.
Contrary to radiation problem, diffraction potential problem is quite complex to solve. First, correct second order body boundary velocity should be derived for the diffraction problem, including the elastic modes. In sequence, the fully coupled diffraction potential-induced pressures and excitations are achieved in the second order hydroelastic analysis. For example, Malenica and Hauteclocque (2012) addressed a fixed elastic cylinder case.
Following definition from Kim and Yue (1990), second order wave excitations are given as

$$F_{ex}^{(2)} = F_I^{(2)} + F_D^{(2)} + F_q^{(2)}, \tag{6}$$

which consists of second order potential-induced loading and first order potential-induced quadratic terms. Focusing on time-domain based second-order hydro-elastic analysis, among the two remaining terms in the second order loadings than the wave excitation, the second order hydrostatic loading, in particular, presents that hydrostatic restoring term in Eq. 3 is identical in both of linear and second order analyses.
Therefore, second order hydro-elastic dynamic analysis in time domain can be conducted for irregular waves by adopting the two-term Volterra series after obtaining fully coupled second order wave excitations.

$$\begin{aligned} F_h^{(1)}(t) &= \mathrm{Re}\sum_a^N \left[A_a f_a^h e^{i\omega_a t} \right] \\ F_h^{(2)}(t) &= \mathrm{Re}\sum_a^N \sum_b^N \left[A_a A_b^* f_{ab}^{h-} e^{i(\omega_a - \omega_b)t} + A_a A_b^* f_{ab}^{h+} e^{i(\omega_a + \omega_b)t} \right] \end{aligned} \tag{7}$$

, where h is index same as i in Eq. 3.

NUMERICAL RESULTS

Hydro-elastic dynamic analysis program for a large floating elastic body has been developed in both frequency and time domains (Kang et al. 2012). In particular, the calculations include shear forces and bending moments at specified sections of the body. The two independently developed programs are cross-checked to each other. For a case study, a simple pontoon-type elastic barge is investigated with 80 (L) x 10 (B) x 5 (D) m; four different bending stiffness cases of infinity, 2.56E10 Nm^2 (Full EI), 1.28E10 Nm^2 (Half EI) , and 6.4E09 Nm^2 (Quarter EI) are investigated with Euler-Bernoulli beam theory, and the most flexible two cases compared between linear and second order analyses. A JONSWAP spectrum with Hs=5, Tp=10.6, and Gamma=1.6 is used as an input wave spectrum.
For both of Half EI and Quarter EI cases, resonances occurred at the first elastic modes in second order analysis. In case of Quarter EI, it has resonance even in linear analysis due to its relatively low natural frequency, and that resonance get more amplified in second order analysis due to sum-frequency force; demonstrated in Fig. 2 ~ 4. The natural frequencies about 1.25 rad/sec and 1.77 rad/sec of Quarter EI and Half EI are for "dry-hull" natural frequency. After including hydrostatic-stiffness and added-mass effects, they changed to about 1.4 rad/sec and 1.68 rad/sec, respectively, as given in Fig. 2.

As a preliminary study, rigid body motion-induced second order excitations are only applied. This is practically acceptable unless high accuracy is needed since the elastic-response contribution in the body-boundary condition of the second-order problem is expected to be an order-of-magnitude smaller than that from rigid-body responses. After including the second-order sum-frequency wave loading, the elastic responses are significantly increased at the lowest-elastic-mode natural frequency, as can be seen in both spectral and time-series analyses. In further study, the complete solution of second order hydro-elastic dynamic analysis will be found, especially for the fully coupled second order excitations of a floating elastic body.

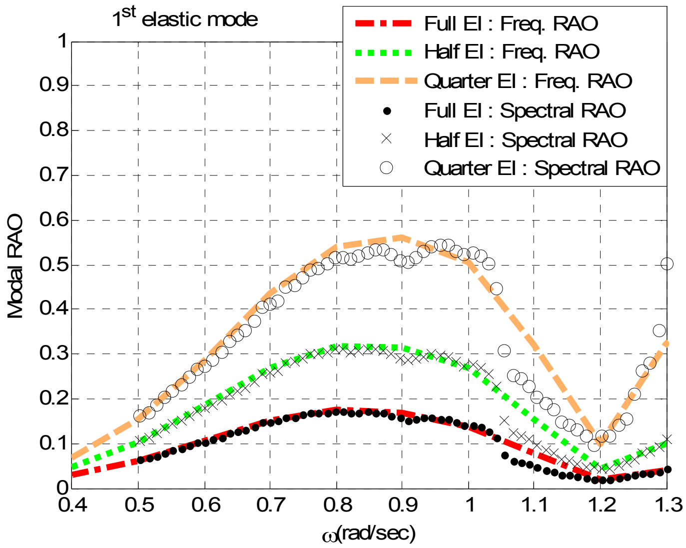

Figure 1 Confirmation by spectral RAO comparison in linear waves

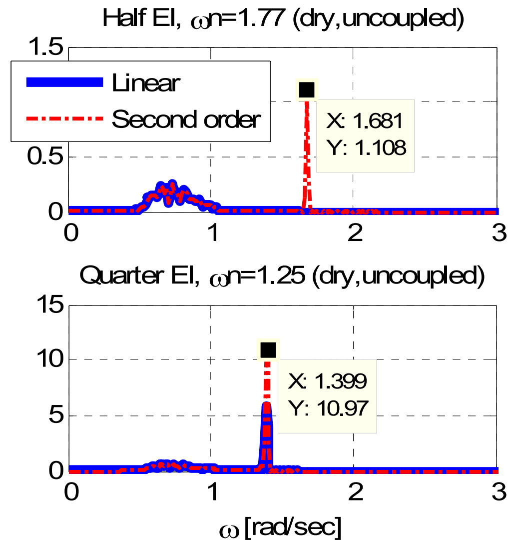

Figure 2 Spectral comparison between 1st and 2nd order for resonance

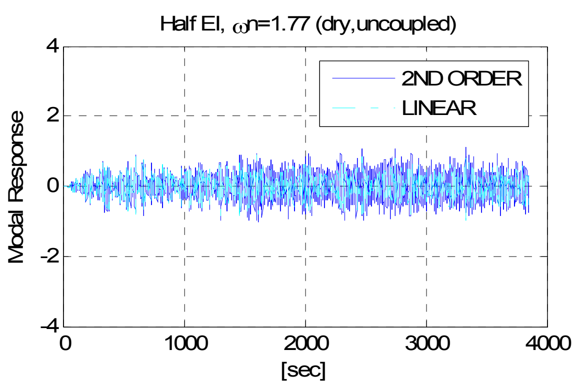

Figure 3 Time series comparison Half EI

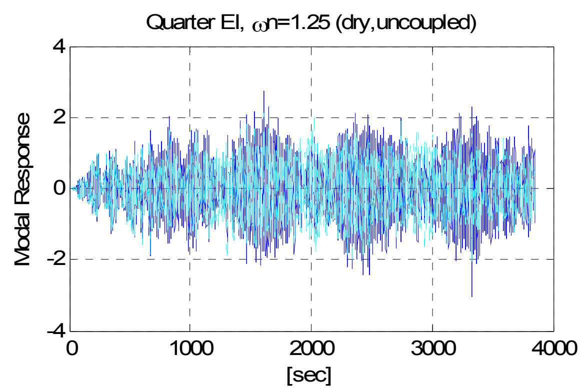

Figure 4 Time series comparison for Quarter EI

REFERENCES

Kang, HY, Kim, MH, Kim, MK, Cho, CY (2012). "Hydroelastic dynamic analysis of large-scale flexible offshore platforms," Proc 22nd ISOPE, Greece, Vol. 1, pp. 967-974.

Kim, MH and Yue, DKP (1989). "The complete second-order diffraction solution for an axisymmetric body. Part 1. Monochromatic incident waves," Journal of Fluid Mechanics, Vol. 200, pp. 235-264.

Kim, MH and Yue, DKP (1990). "The complete second-order diffraction solution for an axisymmetric body. Part 2. Bichromatic incident waves and body motions," Journal of Fluid Mechanics, Vol. 211, pp. 557-593.

Malenica, S. & De Hauteclocque G. (2012). "Second order hydroelastic response of the vertical circular cylinder to monochromatic water waves," 27thIWWWFB, Copenhagen, Denmark.

Molin, B (1979). "Second order diffraction loads upon three dimensional bodies," Applied Ocean Research, Vol. 1, pp. 197-202.